

## ORIGINAL ARTICLE

# Protein phosphatase 6 promotes stemness of colorectal cancer cells

Nobuyuki Fujiwara<sup>1,2</sup> | Ryouichi Tsunedomi<sup>1,3</sup>  | Yuta Kimura<sup>1</sup> | Masao Nakajima<sup>1</sup> | Shinobu Tomochika<sup>1</sup> | Shuhei Enjoji<sup>4</sup> | Takashi Ohama<sup>3,4</sup>  | Koichi Sato<sup>3,4</sup> | Hiroaki Nagano<sup>1,3</sup> 

<sup>1</sup>Department of Gastroenterological, Breast and Endocrine Surgery, Graduate School of Medicine, Yamaguchi University, Ube, Japan

<sup>2</sup>Laboratory of Drug Discovery and Pharmacology, Faculty of Veterinary Medicine, Okayama University of Science, Imabari, Japan

<sup>3</sup>Research Institute for Cell Design Medical Science, Yamaguchi University, Ube, Japan

<sup>4</sup>Laboratory of Veterinary Pharmacology, Faculty of Veterinary Medicine, Yamaguchi University, Yamaguchi, Japan

## Correspondence

Ryouichi Tsunedomi, Department of Gastroenterological, Breast and Endocrine Surgery, Yamaguchi University Graduate School of Medicine, 1-1-1 Minami-Kogushi, Ube, Yamaguchi 755-8505, Japan.  
Email: [tsune-r@yamaguchi-u.ac.jp](mailto:tsune-r@yamaguchi-u.ac.jp)

## Funding information

Japan Society for the Promotion of Science, Grant/Award Number: KAKENHI/21K16434 and KAKENHI/22K08850

## Abstract

Colorectal cancer (CRC) remains a significant global health concern, demanding a more profound comprehension of its molecular foundations for the development of improved therapeutic strategies. This study aimed to elucidate the role of protein phosphatase 6 (PP6), a member of the type 2A protein phosphatase family, in CRC. Protein phosphatase 6 functions as a heterotrimer with a catalytic subunit (PP6c), regulatory subunits (PP6Rs; PP6R1, PP6R2, and PP6R3), and scaffold subunits (ANKRD28, ANKRD44, and ANKRD52). Elevated PP6c expression has been identified in CRC tissues compared to normal mucosa, aligning with its potential involvement in CRC pathogenesis. PP6c knockdown resulted in decreased colony-forming ability and in vivo proliferation of various CRC cell lines. Transcriptome analysis revealed that PP6c knockdown resulted in altered expression of genes associated with cancer stemness. Notably, the PP6c-PP6R3 complex is a key player in regulating cancer stem cell (CSC) markers. Additionally, increased PP6c expression was observed in CSC-like cells induced by sphere formation, implicating the role of PP6c in CSC maintenance. This study highlights the role of PP6c in CRC and suggests that it is a potential therapeutic target disrupting a pathway critical for CRC progression and stem cell maintenance.

## KEYWORDS

cancer stem cell, colony formation, colorectal cancer, protein phosphatase 6, tumor growth

## 1 | INTRODUCTION

Colorectal cancer is one of the most prevalent malignancies worldwide, ranking as the second most lethal cancer with over

916,000 deaths and 1,931,590 cases worldwide in 2020. It was also the third most common cancer worldwide in 2020.<sup>1</sup> Despite the progress of treatment strategy, a significant ratio of CRC patients do not respond well to chemotherapy,<sup>2</sup> and CSCs have

**Abbreviations:** ALDH1A1, aldehyde dehydrogenase 1 family member A1; CRC, colorectal cancer; CSC, cancer stem cell; DEG, differentially expressed gene; EpCAM, epithelial cell adhesion molecule; GSEA, gene set enrichment analysis; IFN, interferon; IRF, interferon regulator factor; NT, nontarget; PP, protein phosphatase; PP6c, PP6 catalytic subunit; PP6R, PP6 regulatory subunit; RNA-seq, RNA sequencing; SIM, sphere induction medium; VCP, valosin-containing protein.

This is an open access article under the terms of the [Creative Commons Attribution-NonCommercial](https://creativecommons.org/licenses/by-nc/4.0/) License, which permits use, distribution and reproduction in any medium, provided the original work is properly cited and is not used for commercial purposes.

© 2024 The Author(s). *Cancer Science* published by John Wiley & Sons Australia, Ltd on behalf of Japanese Cancer Association.

been suggested as potential contributors to this resistance. CSCs represent a subset of cells within a tumor with stem cell characteristics,<sup>3</sup> demonstrating resistance to radiation therapy and chemotherapy while being associated with CRC recurrence and metastasis.<sup>4</sup> Specific marker proteins, including ALDH1A1, CD24, CD44, CD133, EpCAM, and LGR5 are used to identify CSCs in CRC.<sup>5</sup> Considering these features of CSCs, targeting them with agents could potentially reduce CRC recurrence and metastasis.<sup>6</sup> Inflammatory signals such as IFN- $\alpha$  and IFN- $\gamma$  have been implicated in the maintenance of CSCs and the conversion of non-CSCs to CSCs.<sup>7-9</sup> However, the detailed regulatory mechanisms of CSCs remain unclear, and a reliable therapeutic target for CSCs has not yet been identified.

Protein phosphatase 6 is a member of the type 2A Ser/Thr protein phosphatase family.<sup>10</sup> PP6 functions as a heterotrimer with a catalytic subunit (PP6c), regulatory subunits (PP6R1, PP6R2, and PP6R3), and scaffold subunits (ANKRD28, ANKRD44, and ANKRD52).<sup>10</sup> We and other groups reported that PP6 is involved in the regulation of various intracellular signals, such as cell cycle, autophagy, and DNA repair.<sup>11-13</sup> Recent investigations using PP6c KO mice indicated that the PP6c deficiency exacerbates the pathogenesis of skin, pancreatic, and tongue cancers.<sup>14-17</sup> Furthermore, mutational landscape analyses revealed that approximately 10% of melanoma patients harbor nonsynonymous PP6c gene mutations that are presumed to be loss-of-function.<sup>18</sup> These findings suggest that PP6c functions as a cancer suppressor. However, contradictory results have been obtained from studies using human clinical samples.<sup>19,20</sup> Increased PP6c expression in malignant mesotheliomas and gliomas and a negative correlation between PP6c expression and prognosis for gliomas suggest that PP6c functions as a cancer-promoting factor. Increased PP6c expression was observed in patients with inflammatory bowel disease.<sup>21</sup> Inflammatory bowel disease often progresses to CRC; however, there have been no reports on the expression or role of PP6 in CRC.

This study aimed to elucidate the role of PP6 in CRC. Our results showed that PP6c expression was upregulated in CRC and CSC-like cells. The suppression of PP6c expression decreased the expression of CSC markers and reduced colony-forming ability.

## 2 | MATERIALS AND METHODS

### 2.1 | Colorectal cancer tissues used for western blotting, ethics, consent, and permissions

Colorectal cancer tissues from 13 patients were surgically obtained. Tissues were snap-frozen in liquid nitrogen and stored at  $-80^{\circ}\text{C}$ . All patients underwent cancer therapy at Yamaguchi University Hospital. Written informed consent was obtained

from all the patients. This study was approved by the Institutional Review Board of Yamaguchi University Hospital (approval no. H20-102, H23-135, and H28-074) and was conducted following the Declaration of Helsinki.

### 2.2 | Animals and xenograft CRC cell lines

NOD-Rag1<sup>null</sup> IL2r $\gamma$ <sup>null</sup> double mutant mice (NRG mice) were purchased from Jackson Laboratory and maintained in a HEPA-filtered environment with autoclave-sterilized cages, food, and bedding. All animal experiments were carried out in compliance with the Institutional Animal Care and Use Committee of Yamaguchi University (approval no. 33-001).

For the xenograft CRC cell line, a total of  $3 \times 10^5$  Colo205 cells or WiDr cells were xenografted into the hind legs of NRG mice. Tumors were measured using a caliper, and the tumor volume was calculated as  $([\text{width} + \text{length}]/4)3 \times 3 \times 4/3$ .

### 2.3 | Cell culture, sphere induction, and CD133<sup>+</sup> cell isolation

Lenti-X 293T (Takara Bio), HCT116 (ATCC), SW480 (ATCC), and WiDr (RIKEN BioResource Center) cells were grown in DMEM supplemented with 10% FBS and 1 $\times$  antibiotic/antimycotic solution (Thermo Fisher Scientific). Colo205 cells (RIKEN BioResource Center) were grown in RPMI supplemented with 10% FBS and 1 $\times$  antibiotic/antimycotic solution. The sphere was induced by suspension in a SIM. The SIM composition has been described in a previous study.<sup>22-24</sup> CD133<sup>+</sup> cells were isolated from HCT116 and WiDr cells by magnetic cell sorting, using the MACS system (Miltenyi Biotec).

### 2.4 | Plasmids, transfection, virus production, and siRNAs

The shRNA-expressing plasmids were generated as previously described.<sup>11</sup> To produce lentiviruses, 3  $\mu\text{g}$  pLVSIIN, 2.3  $\mu\text{g}$  of a packaging plasmid (psPAX2), and 1.3  $\mu\text{g}$  of a coat protein plasmid expressing vesicular stomatitis virus G protein (pMD2.G) were transfected into Lenti-X 293T cells cultured in 60mm dishes. Viral supernatants were collected after 48 h, filtered (0.22  $\mu\text{m}$ ), and added to Colo205, HCT116, SW480, and WiDr cells for 16 h. Nontargeting siRNA and PP6R1, PP6R2, and PP6R3 targeting siRNA were obtained from Dharmacon (siGENOME Non-Targeting siRNA Pool #1 SiGENOMNE Human PPP6R1 siRNA-SMARTpool, SiGENOMNE Human PPP6R2 siRNA-SMARTpool, and SiGENOMNE Human PPP6R3 siRNA-SMARTpool). siRNA at a final concentration of 10 nM was transfected into cells using

Lipofectamine RNAi Max (Thermo Fisher Scientific) according to the manufacturer's instructions.

## 2.5 | Immunoprecipitation and immunoblotting

For immunoprecipitation, cells stably expressing 3× FLAG-tagged PP6c were lysed in Triton X lysis buffer (50mmol/L Tris-HCl [pH8.0], 150mmol/L NaCl, 5mmol/L EDTA, 5mmol/L EGTA, 1% Triton X-100, 1mmol/L Na<sub>3</sub>VO<sub>4</sub>, 20mmol/L sodium pyrophosphate, and Roche complete protease inhibitor mixture). The supernatants were incubated with FLAG-M2 affinity gel (Sigma-Aldrich). For immunoblotting, CRC and paired nontumor tissues were lysed in T-PER Tissue Protein Extraction Reagent (Thermo Fisher Scientific) supplemented with Halt Protease Inhibitor Cocktail (Thermo Fisher Scientific) using a Qiagen TissueLyser. The cells were lysed in a buffer containing 50mM Tris-HCl (pH8.0), 5mM EDTA, 5mM EGTA, 1% Triton X-100, 1mM Na<sub>3</sub>VO<sub>4</sub>, 20mM sodium pyrophosphate, and a complete protease inhibitor mixture (Roche Diagnostics). Ten micrograms was subjected to SDS-PAGE. Proteins were separated by SDS-PAGE and transferred onto a PVDF membrane (Bio-Rad). Membranes were blocked with 3% skim milk and treated with primary Abs, and immunoreactive bands were visualized using an ECL Pro (PerkinElmer) and Amersham imager 680 (GE Healthcare). Band densities were quantified using the ImageJ densitometry analysis software (NIH). The following Abs were used: anti-ALDH1A1 (15910-1-AP; Proteintech), anti-CD133 (66666-1-Ig; Proteintech), anti-PP2A (07-324; Millipore), anti-FLAG (F7425; Sigma-Aldrich), anti-p62 (PM-045; MBL), anti-PP6c (NBP-13804; Novus), anti-VCP (GTX113030; Gene Tex), anti-PP6R2 (970; Bethyl), and anti-PP6R3 (972; Bethyl). Anti-PP6R1 Ab was kindly provided by Dr. Brautigan (University of Virginia). All Abs were diluted 1/1000. Valosin-containing protein was used as the loading control because its levels are more stable compared to those of other loading controls, such as GAPDH and β-actin.<sup>11,25</sup>

## 2.6 | Colony formation and soft agar colony formation assays

For the colony formation assay,  $3.0 \times 10^2$ – $1.0 \times 10^3$  cells were seeded in 6-well dishes. After 1 week, the cells were fixed with 99.5% ethanol, colonies were stained with Giemsa Stain Solution, and the number of colonies was counted. For the soft agar colony formation assay, a 6-well plate was covered with 2.5mL bottom agar (DMEM containing 10% FBS, 2.8% NaHCO<sub>3</sub>, 1× antibiotic/antimycotic, and 0.75% agarose) and solidified by cooling at 4°C. Cells ( $3 \times 10^3$ ) with 1.5mL top agar (DMEM containing 10% FBS, 2.8% NaHCO<sub>3</sub>, 1× antibiotic/antimycotic, and 0.36% agarose) was added. After 3 weeks of culture, the cells were stained with crystal violet, and the number of colonies was counted.

## 2.7 | Quantitative real-time PCR

The mRNA expression was examined by reverse transcribed quantitative real-time PCR as described previously.<sup>26</sup> Total RNA was extracted from the cells using the RNeasy Mini Kit (Qiagen). RNA (0.5 μg) was reverse-transcribed in a final incubation volume of 10 μL using the PrimeScript RT reagent Kit (Takara Bio). The resulting cDNA was subjected to quantitative PCR using a LightCycler 480 SYBR Green I Master (Roche Diagnostics) and LightCycler System (Roche Diagnostics). The primer sequences were as follows: PP6c forward 5-AGCAAAGGTCACAAATGAGT-3, reverse 5-CATACTGTCACCAGCTTCTC-3; CD44 forward 5-GCAGTCAACAGTCGAAGAAGG-3, reverse 5-TGTCCTCCA CAGCTCCATT-3; and GAPDH forward 5-AGCCACATCGCTC AGACAC-3, reverse 5-GCCCAATACGACCAAATCC-3. The PP6c and CD44 expression levels were normalized to the GAPDH expression levels. The relative quantitative values for PP6c and CD44 compared to GAPDH were expressed using the  $\Delta/\Delta$  threshold cycle method.

## 2.8 | RNA sequencing

Total RNA was isolated using the miRNeasy Mini Kit (Qiagen). Sequencing libraries were constructed using TruSeq Stranded Total RNA with a Ribo-Zero Gold LT Sample Prep Kit (Illumina) according to the manufacturer's instructions. The paired-end fragments were sequenced using the NextSeq 500 sequencing platform (Illumina). After quality control, filtered short reads were mapped to the reference genome (hg38) using STAR (version 2.5.1b).<sup>27</sup> Strand-specific fragment counts were obtained using RSEM (version 1.3.3)<sup>28</sup> followed by removal of genes with low counts and normalized with the trimmed mean of M-values method<sup>29</sup> using the TCC package.<sup>30,31</sup> The edgeR package (version 3.28.1)<sup>32,33</sup> was used to identify DEGs. Differentially expressed genes were recognized based on a false discovery rate *q* value threshold of <0.05, a change of more than two-fold, means of read counts in the higher group >50, and coefficient of variation of each group <1. Gene set enrichment analysis was undertaken with a Java command line program, GSEA2 (version 2.2.1), and Molecular Signatures Database version 7.4.<sup>34</sup>

## 2.9 | Statistical analysis

The results are expressed as mean ± SD. Student's *t*-test was used to compare two groups. Groups of more than three were compared using one-way ANOVA, after which Fisher's least significant difference test was used. For all analyses, a probability value of *p* < 0.05 was considered statistically significant. Each experiment was repeated at least three times.

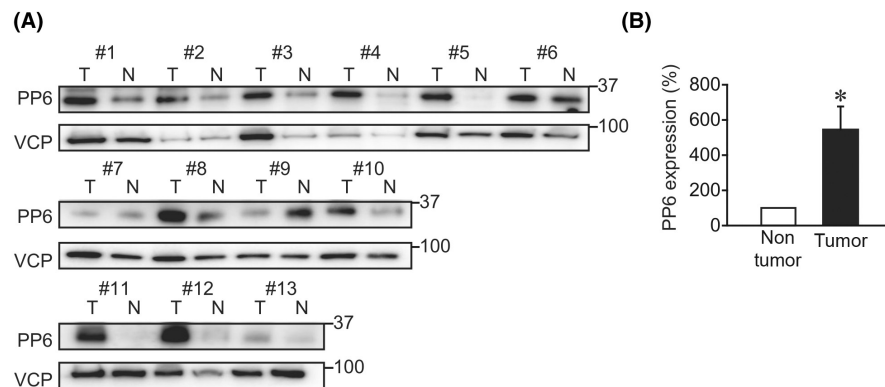


**FIGURE 1** Protein phosphatase 6 catalytic subunit (PP6c) protein is increased in colorectal cancer (CRC). (A) CRC tissues (T) and paired normal tissues (N) were subjected to immunoblotting analysis of PP6c protein level. (B) For quantitative data, the band densities of the tumor tissues were normalized to those of paired normal tissues as 100%. \* $p < 0.05$ . VCP, valosin-containing protein.

### 3 | RESULTS

#### 3.1 | PP6c protein expression is increased in CRC

Although Castellanos-Rubio et al. reported that PP6c expression is increased in inflammatory bowel disease, there are no reports on the role of PP6c in CRC, which often develops due to inflammation.<sup>21</sup> Therefore, proteins were extracted from CRC tissues and paired nontumor tissues, and the expression level of PP6c was examined by western blotting. The results showed that PP6c expression was significantly upregulated in CRC tissues compared to nontumor tissues (Figure 1A,B).

#### 3.2 | PP6c knockdown suppressed colony formation ability and in vivo tumor growth

To elucidate the role of PP6c in CRC, PP6c levels were knocked down in CRC cells by expressing shRNA targeting PP6c (shPP6c #1, shPP6c #2) in CRC cell lines (Colo205, HCT116, SW480, and WiDr) (Figure 2A). These cell lines were used to carry out soft agar colony formation assays (HCT116 and SW480) or colony formation assays (Colo205 and WiDr) (Figure 2B,C). PP6c knockdown decreased the colony number in all cell lines. Furthermore, PP6c knockdown inhibited the in vivo tumor growth of Colo205 and WiDr cells in a xenograft model (Figure 2D,E).

#### 3.3 | PP6c regulates CSC markers

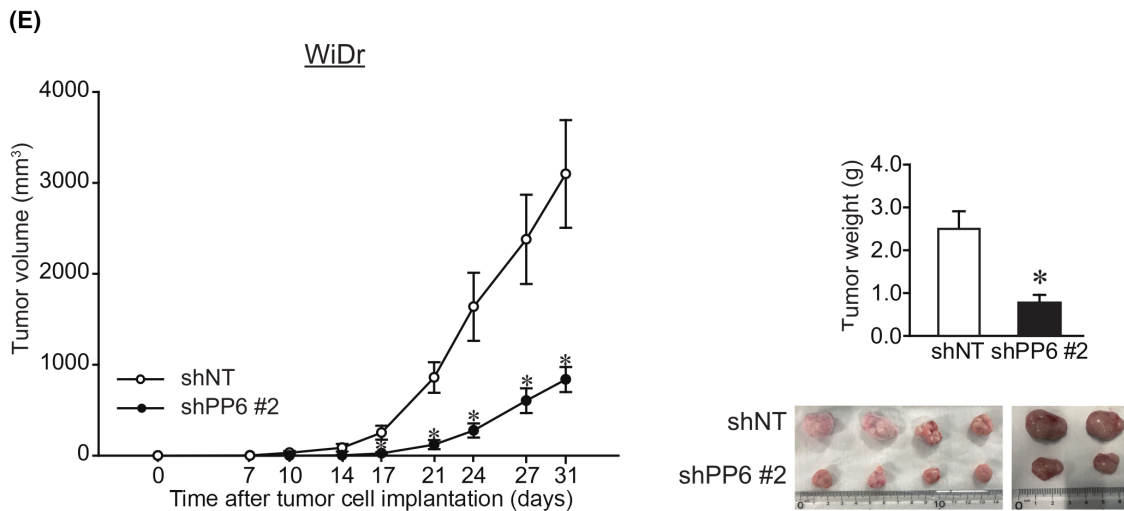
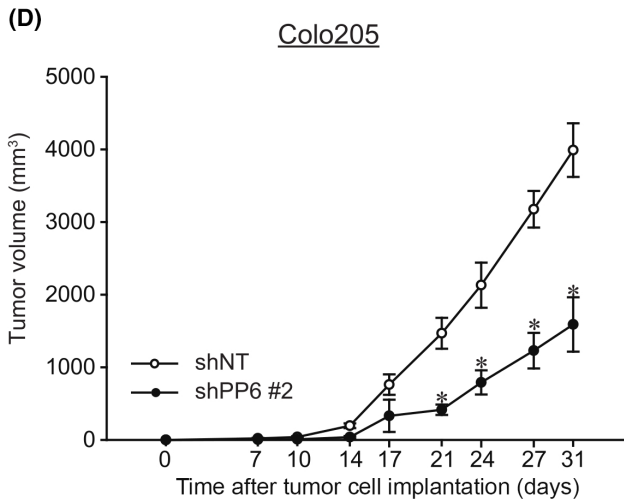
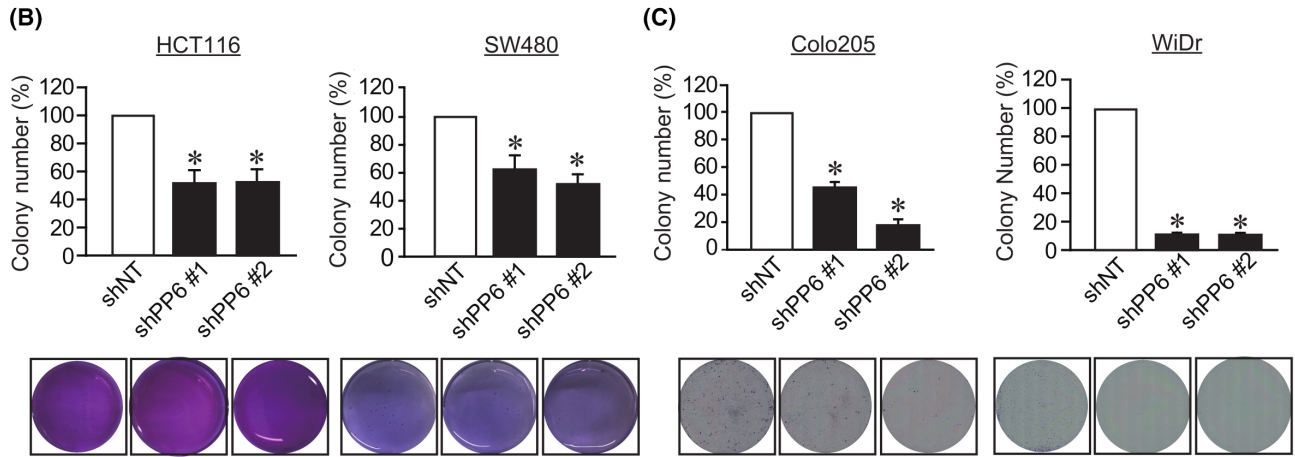
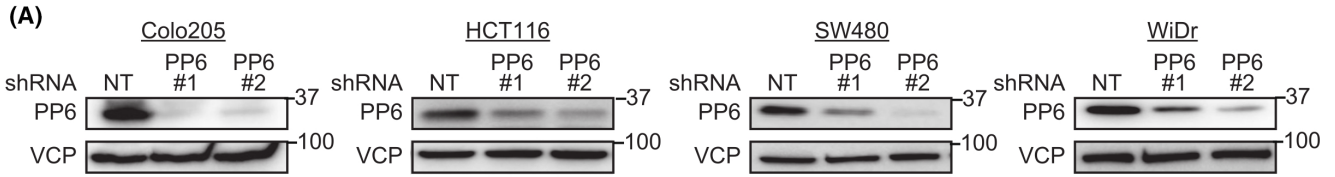
To elucidate the mechanism by which PP6c causes malignant transformation of CRC, RNA-seq analysis was carried out for WiDr cells

expressing shNT and shPP6c #2. Ninety-five DEGs (31 upregulated and 64 downregulated genes, including PP6c) were identified in the read counts between WiDr cells expressing shNT and shPP6c #2 (Figure 3A). A heatmap analysis using the top 50 genes with the lowest  $q$  values well-classified shNT and shPP6c #2 (Figure 3B). We focused on ALDH1A1, which is known as a CSC marker and has the highest A value based on read counts (Figure 3A). The transcripts per million of ALDH1A1 showed the highest among the DEGs (data not shown). Among the other CSC markers (CD24, CD44, CD133, EpCAM, and LGR5),<sup>5</sup> the expression of CD133 was significantly decreased (Figure 3C). GSEA with the mRNA expression profiles of WiDr cells expressing shNT and shPP6c #2 revealed the negatively enriched signatures of IFN- $\alpha$  and IFN- $\gamma$  response gene sets by PP6c knockdown (Figure 3D,E). Because IFN- $\alpha$  and IFN- $\gamma$  response genes are pivotal for CSC maintenance,<sup>7-9</sup> these data suggest that suppression of PP6c expression reduces cancer stemness.

#### 3.4 | PP6c-PP6R3 complex regulates ALDH1A1 and CD133 protein expression

Consistent with the decreased mRNA expression of ALDH1A1 and CD133 in the RNA-seq analysis, PP6c knockdown decreased the protein levels of ALDH1A1 and CD133 in WiDr and HCT116 cells (Figures 4A,B and S1A). In Colo205 and SW480 cells, knockdown of PP6c decreased ALDH1A1 expression, and CD133 expression was not detectable (Figure S1B,C). To exclude the possibility of off-target effects of shRNA, we generated shRNA-resistant PP6c and undertook rescue experiments. Expression of FLAG-PP6c WT restored ALDH1A1 and CD133 expression to the levels of shNT-expressing

**FIGURE 2** Protein phosphatase 6 catalytic subunit (PP6c) knockdown suppresses colony formation and in vivo tumor growth. (A) Effects of nontargeting shRNA (shNT) and PP6c targeting shRNA (shPP6c #1, shPP6c #2) were determined by immunoblotting. Valosin-containing protein (VCP) was used as a loading control. (B) Soft agar colony formation assay was performed to examine anchorage-independent growth. The colony numbers of shPP6c #1 and shPP6c #2 expressing cells were normalized to the colony numbers of shNT expressing cells as 100%. Representative images are shown below. \* $p < 0.05$  versus shNT. (C) Colony formation ability was examined. Colony numbers of shPP6c #1 or shPP6c #2 expressing cells were normalized to colony numbers of shNT expressing cells as 100%. Representative images and quantitative data are shown. \* $p < 0.05$  versus shNT. (D, E) In vivo tumor growth of (D) Colo205 and (E) WiDr cells expressing shNT or shPP6c #2 was examined in a xenograft model ( $n = 6$ ). Tumor growth was monitored by measuring the tumor volume. Tumors were harvested after 30 days of growth, and tumor weights were measured. \* $p < 0.05$ .



cells (Figure 4C,D). In contrast, the FLAG-PP6c H114A mutant, which lacks phosphatase activity, did not restore ALDH1A1 or CD133 expression.<sup>35</sup> Moreover, PP6c WT, but not PP6c H114A, restored the number of colonies (Figure 4E). In clinical samples, when patients were divided into those whose PP6c expression in tumors was increased more than three-fold compared to nontumor and those whose PP6c expression was not, CD133 and ALDH1A1 expressions were elevated in patients with higher PP6c expression in tumor (Figure 4F–H).

The PP6Rs (PP6R1, PP6R2, and PP6R3) recruit PP6c to its substrates. To clarify the involvement of PP6Rs in the regulation of CD133 and ALDH1A1 expression, the expression of PP6R1, PP6R2, and PP6R3 was suppressed using siRNAs. The results showed that ALDH1A1 expression was decreased by PP6R1 and PP6R3 knockdown, and that CD133 expression was decreased by PP6R3 knockdown (Figure 4I,J). Furthermore, among the PP6Rs, only PP6R3 knockdown reduced colony-forming ability (Figure 4K). As colony-forming ability is dependent on cancer stemness,<sup>36</sup> these data suggest that the PP6c-PP6R3 complex plays a pivotal role in the maintenance of CSCs.

### 3.5 | PP6c protein expression is increased in CSC-like cells

As our observations showed that PP6c is involved in the regulation of CSC marker expression, we analyzed the expression level of PP6c in CSCs. SIM has been shown to induce CSC-like cells in cultured cell lines.<sup>22–24</sup> The four CRC cell lines were cultured in SIM to induce CSC-like cells (Figure S2). ALDH1A1 and CD133 proteins and CD44 mRNA expression were upregulated by culturing in SIM, suggesting that SIM induces CSC-like cells in the CRC cell lines. The protein expression level of PP6c was increased in colorectal CSC-like cells (Figure 5A,B). We also found upregulation in the protein expression of all PP6Rs (Figure S3). However, the expression of PP2A, another type 2A protein phosphatase, was not upregulated. Although the mRNA expression of PP6c was upregulated in CSC-like cells (Figure 5C), the increase in PP6c mRNA was less pronounced compared to protein expression, suggesting the suppression of PP6c degradation. PP6c is degraded by p62-mediated selective autophagy.<sup>35</sup> The binding of PP6c to p62 was decreased in CSC-like cells (Figure 5D,E), indicating that PP6c degradation may be suppressed in CSC-like cells. It was also

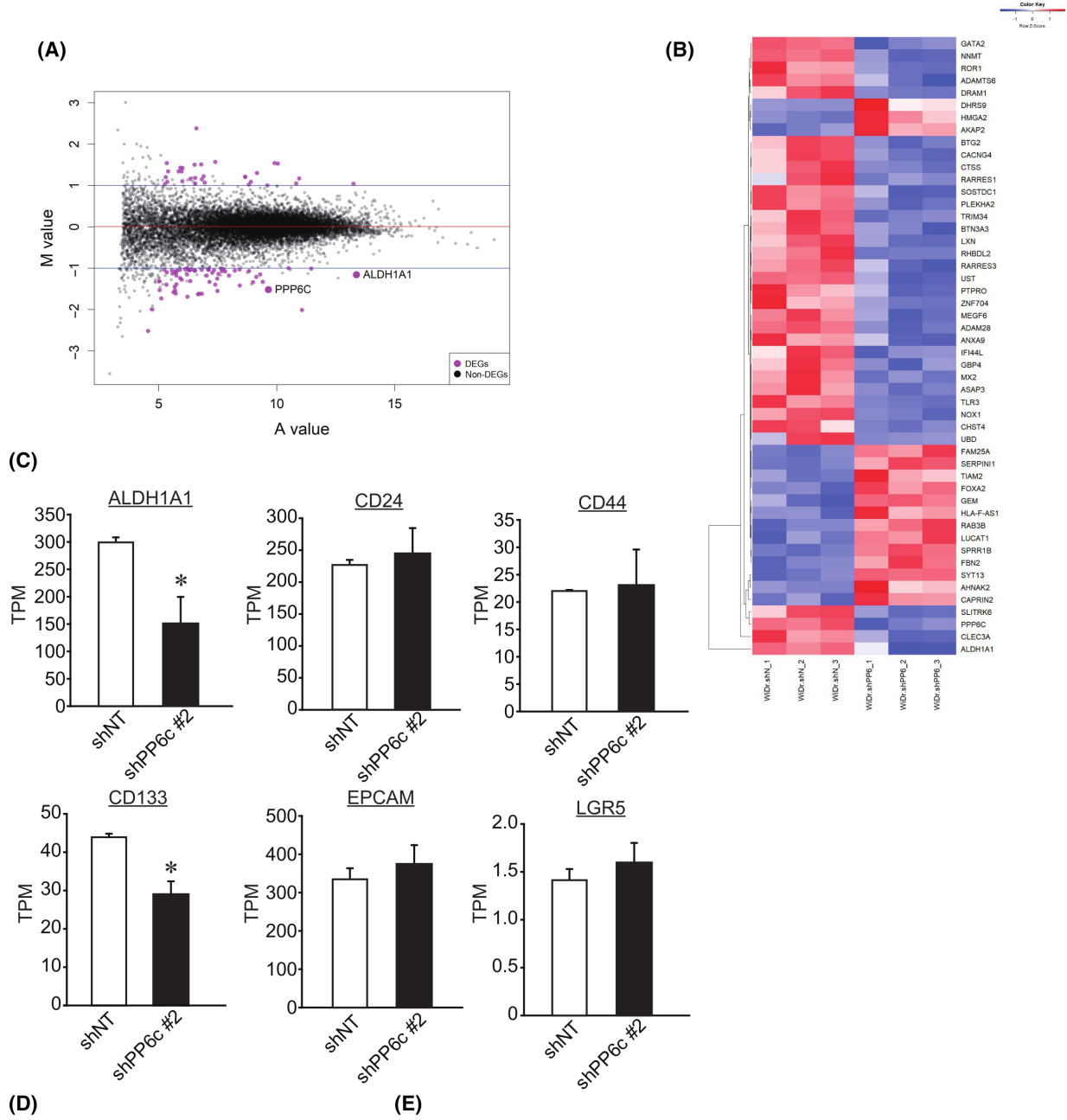
observed that p62 expression was elevated in tumors compared with that in nontumors (Figure 5F,G). This suggests that p62-mediated selective autophagy is suppressed as part of the mechanism by which PP6c expression is elevated in tumors. Moreover, CD133<sup>+</sup> cells were isolated from HCT116 and WiDr cells to examine the protein level of PP6c. Consistent with the previous data, PP6c protein levels were higher in CD133<sup>+</sup> cells compared to CD133<sup>-</sup> cells (Figure 5H,I). Finally, sphere formation assay revealed that the PP6c knockdown reduced the number of spheres formed (Figure 5J) and reduced the viability of cells in SIM (data not shown). These data indicate that PP6c plays a pivotal role in colorectal CSCs.

## 4 | DISCUSSION

This study aimed to examine the function of PP6c in CRC, specifically focusing on its expression and impact on CSCs. Our findings revealed substantial upregulation of PP6c expression in CRC tissues compared to normal colonic mucosa, implying a potential link between PP6c and CRC pathogenesis. Notably, the elevated expression of PP6c in CRC aligns with previous observations in inflammatory bowel disease, a recognized precursor to CRC.<sup>21</sup> The increase in PP6c expression was reported in other cancers, such as glioma and malignant mesotheliomas.<sup>19,20</sup> However, studies using KO mice have reported that the loss of PP6c exacerbates the pathogenesis of skin, tongue, and pancreatic cancers.<sup>14,16,17</sup> Therefore, the role of PP6c in cancer may differ during the cancer progression process: PP6c functions as a cancer suppressor at the developmental stage, and as it progresses, it functions as a cancer promotor.

In the present study, PP6c knockdown reduced colony-forming ability in all CRC cell lines with different genetic mutations.<sup>37</sup> The PP6c H114 mutant, which lacks phosphatase activity, failed to restore colony-forming ability and expression of CSC markers, indicating that the enzymatic activity of PP6c is indispensable. Because colony-forming ability has been reported to correlate with *in vivo* proliferation,<sup>38,39</sup> it is expected that PP6c WT rescue will restore *in vivo* proliferation suppressed by PP6c knockdown. Knockdown of PP6R3 resulted in diminished colony-forming ability and CSC marker expression, suggesting that the PP6c-PP6R3 complex plays a crucial role in maintaining stemness regardless of the genetic mutation present in CRC cells. The role of the PP6c-PP6R3 complex in cancer

**FIGURE 3** Protein phosphatase 6 catalytic subunit (PP6c) regulates cancer stem cell (CSC) markers. (A) MA plot of RNA sequencing (RNA-seq) read count data for WiDr cells expressing nontargeting shRNA (shNT) versus shPP6c #2. For each gene, the log<sub>2</sub> (average expression) in the two samples (A, x-axis) against the log<sub>2</sub> (fold change) between the samples was plotted (M, y-axis). Magenta circles represent significant differentially expressed genes (DEGs). Black circles indicate genes that were not significantly different between cells expressing shNT and shPP6c #2. (B) Heatmap of RNA-seq for WiDr cells expressing shNT vs. shPP6c #2. (C) Graphical representation of transcripts per million (TPM) of CSC markers. \**p* < 0.05. (D, E) Gene set enrichment analysis of (D) HALLMARK\_INTERFERON\_ARUFA\_RESPONSE and (E) HALLMARK\_INTERFERON\_GAMMA\_RESPONSE gene signatures in the RNA-seq data from WiDr cells expressing shNT or shPP6c #2 (*q* < 0.01). FDR-*q*, false discovery rate-adjusted *q* value; NES, normalized enrichment score.



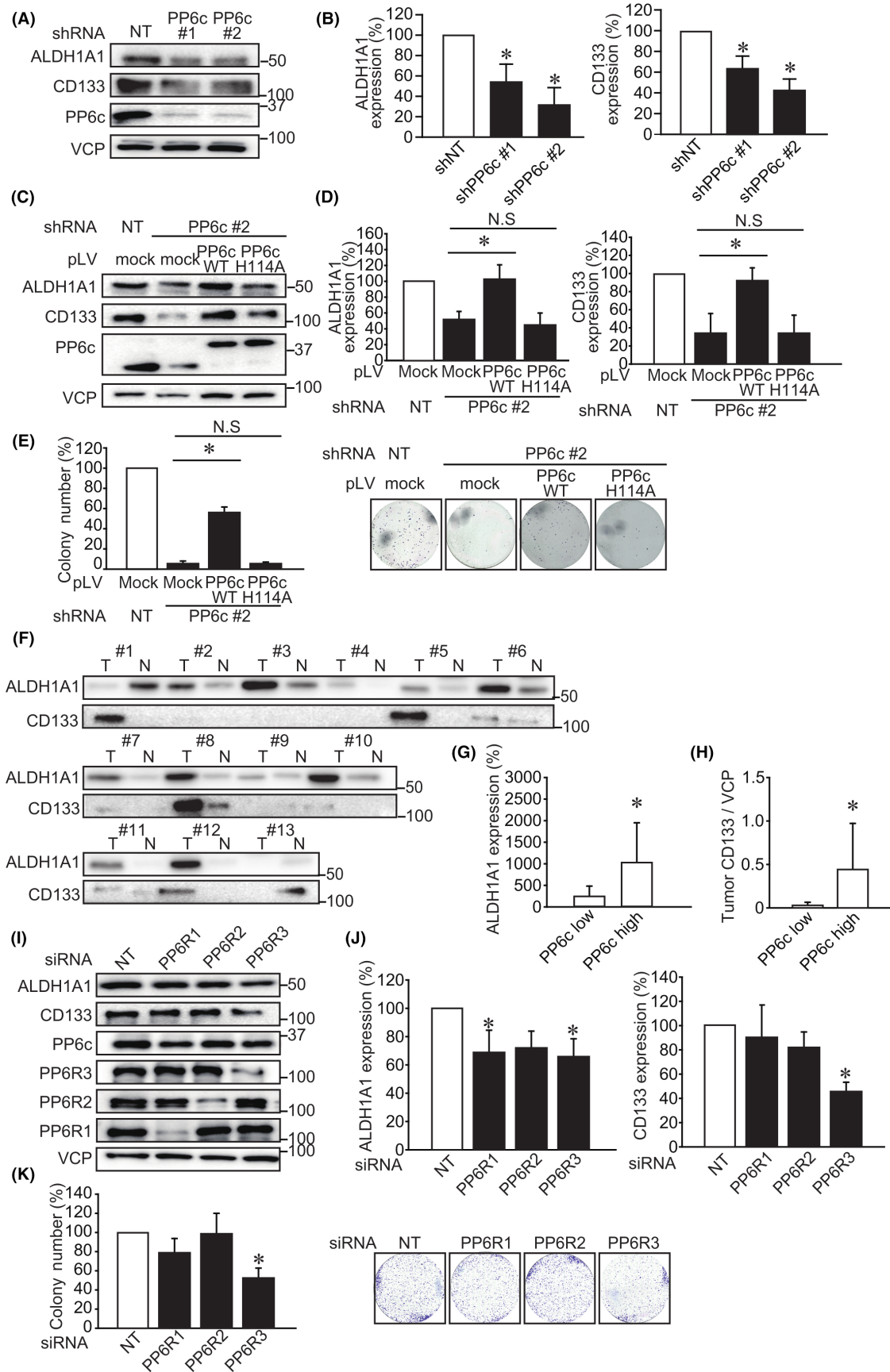


**FIGURE 4** Protein phosphatase 6 catalytic subunit (PP6c)-PP6 regulatory subunit 3 (PP6R3) complex regulates aldehyde dehydrogenase 1 family member A1 (ALDH1A1) and CD133 protein expression. (A, B) WiDr cells stably expressing nontargeting shRNA (shNT), shPP6c #1, or shPP6c #2. ALDH1A1 and CD133 protein levels were detected using immunoblotting. Representative images (A) and quantitative data (B) are shown. \* $p < 0.05$  versus shNT. (C, D) WiDr cells stably expressing shPP6c #2 and shPP6c #2-resistant FLAG-PP6c WT or FLAG-PP6c H114A. Empty vector was used as the mock control. Protein levels of PP6c, ALDH1A1, and CD133 were detected by immunoblotting. Representative images (C) and quantitative data (D) are shown. \* $p < 0.05$ . (E) Colony formation ability was examined in WiDr cells expressing shNT, shPP6c #2, shPP6c #2-resistant FLAG-PP6c WT, or FLAG-PP6c H114A. Representative images are shown at the right. \* $p < 0.05$ . (F) Colorectal cancer tissues (T) and paired normal tissues (N) were subjected to immunoblotting analysis of ALDH1A1 and CD133 protein level. (G, H) Expression levels of ALDH1A1 and CD133 were quantified by dividing patients with a three-fold or greater increase in PP6c expression in tumors compared to nontumors into PP6c high ( $n = 9$ ) and PP6c low ( $n = 4$ ) groups. \* $p < 0.05$ . (I, J) WiDr cells transiently expressing siNT, siPP6R1, siPP6R2, or siPP6R3. ALDH1A1 and CD133 protein level was detected by immunoblotting. Representative images (I) and quantitative data (J) are shown. \* $p < 0.05$  versus shNT. (K) Colony formation ability of WiDr cells expressing siNT, siPP6R1, siPP6R2, or siPP6R3. Colony numbers of siPP6R1, siPP6R2, or siPP6R3 expressing cells were normalized to the colony numbers of siNT expressing cells as 100%. Representative images and quantitative data are shown. \* $p < 0.05$  versus shNT. N.S, not significant; VCP, valosin-containing protein.

has not yet been reported, and this study provides the first evidence of its involvement in cancer.

RNA sequencing analysis revealed that suppression of PP6c expression reduces IFN signaling, which plays an important role in the maintenance of CSCs.<sup>7-9</sup> Although the mechanism has not been clarified in this study, Hou et al. recently reported that PP6c expression in cervical cancer cells is regulated by IRF5, which modulates IFN signaling.<sup>40</sup> It has also been shown that colony-forming ability and cell migration ability, which are reduced by IRF suppression, are restored by PP6c rescue.

Knockdown of PP6c decreased the expression of ALDH1A1 and CD133 mRNAs, indicating that PP6c is involved in the regulation of ALDH1A1 and CD133 at the transcript levels. We also generated PP6c overexpressing cells. However, we could not achieve PP6c overexpression because endogenous PP6c was degraded along with exogenous PP6c (Figure S4). Supporting this, in the rescue experiment, exogenous PP6c expression was only achieved at the same or lower level as shNT transfectants, and the slight remaining endogenous PP6c was diminished (Figure 4C). The difficulties of PP6c overexpression may be due to the regulation of PP6c protein degradation.<sup>35</sup> In this study, the detailed molecular mechanisms by which PP6c promotes the expression of CSC markers remain to be elucidated. One possibility is that PP6c represses Wnt/ $\beta$ -catenin and NFE2-related factor 2 (NRF2) signaling that induces CD133 and ALDH1A1 expression.<sup>41-44</sup> Moreover, the PP6-PP6R3 complex is involved in telomere repair by dephosphorylating Ser365 of TRF2,<sup>45</sup> and in metabolic regulation by dephosphorylating and inactivating AMPK.<sup>46</sup> Therefore, it is considered that multiple factors are involved in the PP6c-mediated induction of CSC marker expression.

Expression of PP6c was markedly enhanced in CSC-like cells induced by sphere formation. Furthermore, suppression of autophagy by treatment with bafilomycin A1 increased the expression of p62 and PP6c, but not that of ALDH1A1 or CD133 (Figure S5). It has been reported that autophagy is activated in CSCs.<sup>47</sup> We

have previously reported that the protein level of PP6c is regulated by p62-mediated selective autophagy.<sup>35</sup> In this study, the decreased binding of PP6c to p62 and the increased PP6c mRNA expression were observed in CSC-like cells. These data suggest that both p62-mediated selective autophagy and transcriptional regulation are involved. The regulatory mechanisms of p62-PP6c binding and the transcriptional regulation of PP6c remains unclear, and further analysis is required to elucidate these points. Recently, Wang et al. reported that the hairy transcription factor and enhancer of split 1 (HES1) promotes the expression of immunoglobulin-binding protein 1 (IGBP1), which binds to PP6c and accumulates PP6c protein by suppressing ubiquitination.<sup>48</sup> Therefore, evasion from the ubiquitin-proteasome system might also be involved in the PP6c protein accumulation. The PP6R proteins were upregulated in CSC-like cells. Knockout/knockdown of PP6c decreases PP6R protein levels, suggesting that PP6c enhances the stability of PP6Rs by forming a holoenzyme.<sup>35,49,50</sup> Therefore, increased PP6c expression might contribute to the PP6Rs accumulation in cancer stem-like cells.

The relationship between the expression levels of PP6c, PP6R1, PP6R2, and PP6R3 and prognosis was analyzed using The Cancer Genome Atlas (TCGA) database (Figure S6). Although the significantly poor prognosis of patients with high PP6R1 was shown, the PP6c expression level was not related to prognosis, and high expression of PP6R3 was associated with better prognosis. We have previously reported that PP6c expression is regulated at the protein level.<sup>35</sup> Therefore, it is necessary to analyze PP6c protein levels in clinical specimens to determine its prognostic relevance.

In conclusion, the study provides valuable insights into the role of PP6c in CRC, shedding light on its expression patterns, functional impact on CSCs, and potential as a therapeutic target. These findings expand our understanding of the intricate molecular landscape of CRC and could facilitate the development of tailored treatments that disrupt the PP6c-PP6R3 complex-mediated pathways in CRC.

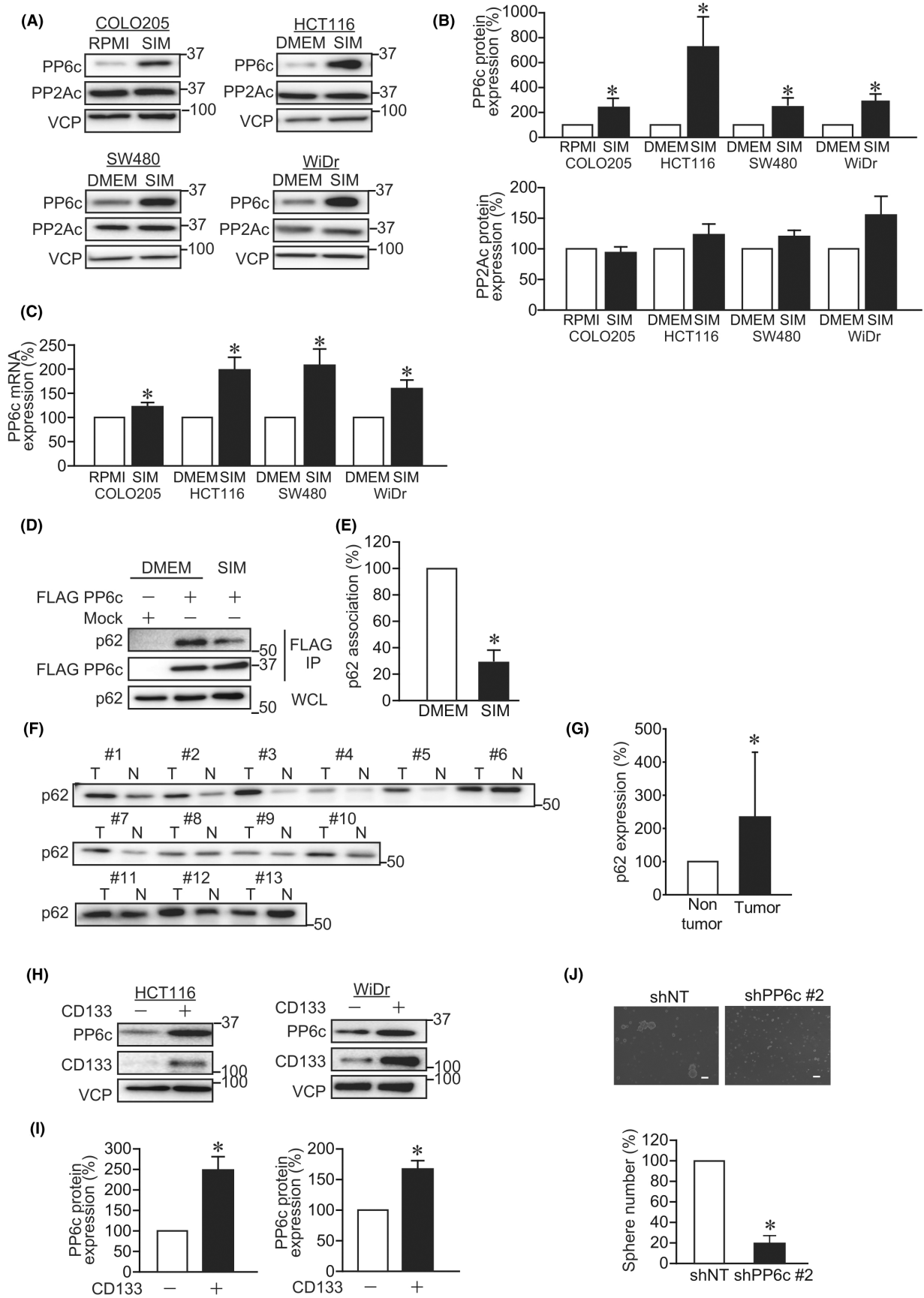


**FIGURE 5** Protein phosphatase 6 catalytic subunit (PP6c) protein expression is increased in cancer stem cell-like cells. (A, B) Colo205, HCT116, SW480, and WiDr cells were suspended in normal medium (RPMI or DMEM) for 2 days or in sphere induction medium (SIM) for 7 days. Protein expression levels of PP6c and PP2A were analyzed by immunoblotting. Representative images (A) and quantitative data (B) are shown. \* $p < 0.05$ . (C) Colo205, HCT116, SW480, and WiDr cells were suspended in normal (RPMI or DMEM) or SIM for 2 days. PP6c mRNA expression levels were quantified using quantitative real-time PCR. \* $p < 0.05$ . (D, E) WiDr cells stably expressing FLAG-PP6c were suspended in DMEM for 2 days or in SIM for 7 days. FLAG-PP6c was immunoprecipitated (IP) using FLAG M2 beads and its association with p62 was analyzed by immunoblotting. Representative images (D) and quantitative data (E) are shown. \* $p < 0.05$ . WCL: Whole cell lysate. (F) Colorectal cancer tissues (T) and paired normal tissues (N) were subjected to immunoblotting analysis of p62 protein level. (G) For quantitative data, the band densities of the tumor tissues were normalized to those of paired normal tissues as 100%. \* $p < 0.05$ . (H, I) HCT116 and WiDr cells were separated into CD133<sup>+</sup> and CD133<sup>-</sup> cells. Protein expression levels of PP6c and CD133 were analyzed by immunoblotting. Representative images (H) and quantitative data (I) are shown. \* $p < 0.05$ . (J) WiDr cells expressing nontargeting shRNA (shNT) or shPP6c #2 were cultured in SIM for 7 days. Sphere numbers of shPP6c #2 expressing cells were normalized to the sphere numbers of shNT expressing cells as 100%. Scale bar, 100  $\mu$ M. \* $p < 0.05$ .

## AUTHOR CONTRIBUTIONS

**Nobuyuki Fujiwara:** Conceptualization; data curation; formal analysis; funding acquisition; investigation; resources; visualization; writing – original draft; writing – review and editing. **Ryouchi Tsunedomi:** Conceptualization; data curation; formal analysis; funding acquisition; methodology; project administration; resources; software; supervision; visualization; writing – original draft; writing – review and editing. **Yuta Kimura:** Data curation; investigation; validation. **Masao Nakajima:** Data curation; validation. **Shinobu Tomochika:** Data curation; validation. **Shuhei Enjoji:** Data curation; validation. **Takashi Ohama:** Conceptualization; data curation; methodology; validation. **Koichi Sato:** Data curation; methodology; validation. **Hiroaki Nagano:** Data curation; writing – review and editing.

## ACKNOWLEDGMENTS

We thank Dr. David L Brautigan for providing us an anti-PP6R1 antibody.

## FUNDING INFORMATION

This work was supported by the Japan Society for the Promotion of Science (KAKENHI grant numbers 21K16434 and 22K08850).

## CONFLICT OF INTEREST STATEMENT

The authors declare no conflict of interest.

## ETHICS STATEMENTS

Approval of the research protocol by an Institutional Review Board: This study was approved by the Institutional Review Board of Yamaguchi University Hospital (Approval No. H20-102, H23-135, and H28-074).

Informed consent: Written informed consent was obtained from all patients.

Registry and the Registration No. of the study/trial: N/A.

Animal studies: All animal experiments were performed in compliance with the Institutional Animal Care and Use Committee of Yamaguchi University (Approval No. 33-001).

## ORCID

Ryouchi Tsunedomi  <https://orcid.org/0000-0003-4251-1936>

Takashi Ohama  <https://orcid.org/0000-0003-2998-6689>

Hiroaki Nagano  <https://orcid.org/0000-0002-7074-3315>

## REFERENCES

1. Cancer. <https://www.who.int/news-room/fact-sheets/detail/cancer>.
2. Van Cutsem E, Cervantes A, Adam R, et al. ESMO consensus guidelines for the management of patients with metastatic colorectal cancer. *Ann Oncol*. 2016;27:1386-1422.
3. Prasad S, Ramachandran S, Gupta N, Kaushik I, Srivastava SK. Cancer cells stemness: a doorstep to targeted therapy. *Biochim Biophys Acta Mol basis Dis*. 2020;1866:165424.
4. Wang H, Cui G, Yu B, Sun M, Yang H. Cancer stem cell niche in colorectal cancer and targeted therapies. *Curr Pharm Des*. 2020;26:1979-1993.
5. Cherciu I, Bărbălan A, Pirici D, Mărgăritescu C, Săftoiu A. Stem cells, colorectal cancer and cancer stem cell markers correlations. *Curr Health Sci J*. 2014;40:153-161.
6. Frank MH, Wilson BJ, Gold JS, Frank NY. Clinical implications of colorectal cancer stem cells in the age of single-cell omics and targeted therapies. *Gastroenterology*. 2021;160:1947-1960.
7. Shigdar S, Li Y, Bhattacharya S, et al. Inflammation and cancer stem cells. *Cancer Lett*. 2014;345:271-278.
8. Musella M, Guarracino A, Manduca N, et al. Type I IFNs promote cancer cell stemness by triggering the epigenetic regulator KDM1B. *Nat Immunol*. 2022;23:1379-1392.
9. Beziaud L, Young CM, Alonso AM, Norkin M, Minafra AR, Huelsken J. IFN $\gamma$ -induced stem-like state of cancer cells as a driver of metastatic progression following immunotherapy. *Cell Stem Cell*. 2023;30:818-831.e6.
10. Ohama T. The multiple functions of protein phosphatase 6. *Biochim Biophys Acta, Mol Cell Res*. 2019;1866:74-82.
11. Fujiwara N, Shibutani S, Ohama T, Sato K. Protein phosphatase 6 dissociates the Beclin 1/Vps34 complex and inhibits autophagy. *Biochem Biophys Res Commun*. 2021;552:191-195.
12. Kajino T, Ren H, Iemura SI, et al. Protein phosphatase 6 downregulates TAK1 kinase activation in the IL-1 signaling pathway. *J Biol Chem*. 2006;281:39891-39896.
13. Stefansson B, Brautigan DL. Protein phosphatase PP6 N terminal domain restricts G1 to S phase progression in human cancer cells. *Cell Cycle*. 2007;6:1386-1392.
14. Hayashi K, Momoi Y, Tanuma N, et al. Abrogation of protein phosphatase 6 promotes skin carcinogenesis induced by DMBA. *Oncogene*. 2015;34:4647-4655.
15. Fukui K, Nomura M, Kishimoto K, et al. PP6 deficiency in mice with KRAS mutation and Trp53 loss promotes early death by PDAC with cachexia-like features. *Cancer Sci*. 2022;113:1613-1624.
16. Kato H, Kurosawa K, Inoue Y, et al. Loss of protein phosphatase 6 in mouse keratinocytes increases susceptibility to ultraviolet-B-induced carcinogenesis. *Cancer Lett*. 2015;365:223-228.
17. Kishimoto K, Kanazawa K, Nomura M, et al. Ppp6c deficiency accelerates K-rasG12D -induced tongue carcinogenesis. *Cancer Med*. 2021;10:4451-4464.

18. Hodis E, Watson IR, Kryukov GV, et al. A landscape of driver mutations in melanoma. *Cell*. 2012;150:251-263.
19. Shen Y, Wang Y, Sheng K, et al. Serine/threonine protein phosphatase 6 modulates the radiation sensitivity of glioblastoma. *Cell Death Dis*. 2011;2:e241.
20. Ivanov SV, Goparaju CMV, Lopez P, et al. Pro-tumorigenic effects of miR-31 loss in mesothelioma. *J Biol Chem*. 2010;285:22809-22817.
21. Castellanos-Rubio A, Martin-Pagola A, Santín I, et al. Combined functional and positional gene information for the identification of susceptibility variants in celiac disease. *Gastroenterology*. 2008;134:738-746.
22. Watanabe Y, Yoshimura K, Yoshikawa K, et al. A stem cell medium containing neural stimulating factor induces a pancreatic cancer stem-like cell-enriched population. *Int J Oncol*. 2014;45:1857-1866.
23. Hashimoto N, Tsunedomi R, Yoshimura K, Watanabe Y, Hazama S, Oka M. Cancer stem-like sphere cells induced from dedifferentiated hepatocellular carcinoma-derived cell lines possess the resistance to anti-cancer drugs. *BMC Cancer*. 2014;14:722.
24. Nishiyama M, Tsunedomi R, Yoshimura K, et al. Metastatic ability and the epithelial-mesenchymal transition in induced cancer stem-like hepatoma cells. *Cancer Sci*. 2018;109:1101-1109.
25. Fujiwara N, Usui T, Ohama T, Sato K. Regulation of Beclin 1 protein phosphorylation and autophagy by protein phosphatase 2A (PP2A) and death-associated protein kinase 3 (DAPK3). *J Biol Chem*. 2016;291:10858-10866.
26. Tsunedomi R, Iizuka N, Tamesa T, et al. Decreased ID2 promotes metastatic potentials of hepatocellular carcinoma by altering secretion of vascular endothelial growth factor. *Clin Cancer Res*. 2008;14:1025-1031.
27. Wang T, Liu J, Shen L, et al. STAR: an integrated solution to management and visualization of sequencing data. *Bioinformatics*. 2013;29:3204-3210.
28. Li B, Dewey CN. RSEM: accurate transcript quantification from RNA-Seq data with or without a reference genome. *BMC Bioinformatics*. 2011;12:323.
29. Robinson MD, Oshlack A. A scaling normalization method for differential expression analysis of RNA-seq data. *Genome Biol*. 2010;11:R25.
30. Sun J, Nishiyama T, Shimizu K, Kadota K. TCC: an R package for comparing tag count data with robust normalization strategies. *BMC Bioinformatics*. 2013;14:219.
31. Tang M, Sun J, Shimizu K, Kadota K. Evaluation of methods for differential expression analysis on multi-group RNA-seq count data. *BMC Bioinformatics*. 2015;16:361.
32. Robinson MD, McCarthy DJ, Smyth GK. edgeR: a Bioconductor package for differential expression analysis of digital gene expression data. *Bioinformatics*. 2010;26:139-140.
33. McCarthy DJ, Chen Y, Smyth GK. Differential expression analysis of multifactor RNA-Seq experiments with respect to biological variation. *Nucleic Acids Res*. 2012;40:4288-4297.
34. Subramanian A, Tamayo P, Mootha VK, et al. Gene set enrichment analysis: a knowledge-based approach for interpreting genome-wide expression profiles. *Proc Natl Acad Sci USA*. 2005;102:15545-15550.
35. Fujiwara N, Shibutani S, Sakai Y, et al. Autophagy regulates levels of tumor suppressor enzyme protein phosphatase 6. *Cancer Sci*. 2020;111:4371-4380.
36. Geng S, Wang Q, Wang J, et al. Isolation and identification of a distinct side population cancer cells in the human epidermal squamous cancer cell line A431. *Arch Dermatol Res*. 2011;303:181-189.
37. Berg KCG, Eide PW, Eilertsen IA, et al. Multi-omics of 34 colorectal cancer cell lines - a resource for biomedical studies. *Mol Cancer*. 2017;16:116.
38. Nie H, Li J, Yang XM, et al. Mineralocorticoid receptor suppresses cancer progression and the Warburg effect by modulating the miR-338-3p-PKLR axis in hepatocellular carcinoma. *Hepatology*. 2015;62:1145-1159.
39. Enjoji S, Yabe R, Tsuji S, et al. Stemness is enhanced in gastric cancer by a SET/PP2A/E2F1 Axis. *Mol Cancer Res*. 2018;16:554-563.
40. Hou P-X, Fan Q, Zhang Q, Liu J-J, Wu Q. M6A-induced transcription factor IRF5 contributes to the progression of cervical cancer by upregulating PPP6C. *Clin Exp Pharmacol Physiol*. 2024;51:e13868.
41. Wei Y, Li Y, Chen Y, et al. ALDH1: a potential therapeutic target for cancer stem cells in solid tumors. *Front Oncol*. 2022;12:1026278.
42. Moreno-Londoño AP, Robles-Flores M. Functional roles of CD133: more than Stemness associated factor regulated by the microenvironment. *Stem Cell Rev Rep*. 2024;20:25-51.
43. Leung HW, Lau EYT, Leung CON, et al. NRF2/SHH signaling cascade promotes tumor-initiating cell lineage and drug resistance in hepatocellular carcinoma. *Cancer Lett*. 2020;476:48-56.
44. Duong H-Q, You KS, Oh S, Kwak S-J, Seong Y-S. Silencing of NRF2 reduces the expression of ALDH1A1 and ALDH3A1 and sensitizes to 5-FU in pancreatic cancer cells. *Antioxidants (Basel)*. 2017;6:52.
45. Sarek G, Kotsantis P, Ruis P, et al. CDK phosphorylation of TRF2 controls t-loop dynamics during the cell cycle. *Nature*. 2019;575:523-527.
46. Yang Y, Reid MA, Hanse EA, et al. SAPS3 subunit of protein phosphatase 6 is an AMPK inhibitor and controls metabolic homeostasis upon dietary challenge in male mice. *Nat Commun*. 2023;14:1368.
47. Li D, Peng X, He G, et al. Crosstalk between autophagy and CSCs: molecular mechanisms and translational implications. *Cell Death Dis*. 2023;14:409.
48. Wang Z, Sun Y, Lou F, et al. Targeting the transcription factor HES1 by L-menthol restores protein phosphatase 6 in keratinocytes in models of psoriasis. *Nat Commun*. 2022;13:7815.
49. Ohama T, Wang L, Griner EM, Brautigan DL. Protein Ser/Thr phosphatase-6 is required for maintenance of E-cadherin at adherens junctions. *BMC Cell Biol*. 2013;14:42.
50. Stefansson B, Ohama T, Daugherty AE, Brautigan DL. Protein phosphatase 6 regulatory subunits composed of ankyrin repeat domains. *Biochemistry*. 2008;47:1442-1451.

## SUPPORTING INFORMATION

Additional supporting information can be found online in the Supporting Information section at the end of this article.

**How to cite this article:** Fujiwara N, Tsunedomi R, Kimura Y, et al. Protein phosphatase 6 promotes stemness of colorectal cancer cells. *Cancer Sci*. 2024;115:3067-3078. doi:[10.1111/cas.16271](https://doi.org/10.1111/cas.16271)